Energies and wave functions for a soft-core Coulomb potential

Richard L. Hall[1], Nasser Saad[2], K. D. Sen[3], and Hakan Ciftci[4]

[1] *Department of Mathematics and Statistics, Concordia University,*
1455 de Maisonneuve Boulevard West, Montréal, Québec, Canada H3G 1M8
[2] *Department of Mathematics and Statistics, University of Prince Edward Island,*
550 University Avenue, Charlottetown, PEI, Canada C1A 4P3.
[3] *School of Chemistry, University of Hyderabad 500046, India. and*
[4] *Gazi Universitesi, Fen-Edebiyat Fakültesi, Fizik Bölümü, 06500 Teknikokullar, Ankara, Turkey.*

For the family of model soft-core Coulomb potentials represented by $V(r) = -\frac{Z}{(r^q+\beta^q)^{\frac{1}{q}}}$, with the parameters $Z > 0$, $\beta > 0$, $q \geq 1$, it is shown analytically that the potentials and eigenvalues, $E_{\nu\ell}$, are monotonic in each parameter. The potential envelope method is applied to obtain approximate analytic estimates in terms of the known exact spectra for pure power potentials. For the case $q = 1$, the Asymptotic Iteration Method is used to find exact analytic results for the eigenvalues $E_{\nu\ell}$ and corresponding wave functions, expressed in terms of Z and β. A proof is presented establishing the general concavity of the scaled electron density near the nucleus resulting from the truncated potentials for all q. Based on an analysis of extensive numerical calculations, it is conjectured that the crossing between the pair of states $[(\nu, \ell), (\nu', \ell')]$, is given by the condition $\nu' \geq (\nu + 1)$ and $\ell' \geq (\ell+3)$. The significance of these results for the interaction of an intense laser field with an atom is pointed out. Differences in the observed level-crossing effects between the soft-core potentials and the hydrogen atom confined inside an impenetrable sphere are discussed.

I. INTRODUCTION

The Schrödinger's time-independent equation $H\Psi = E\Psi$, where the Hamiltonian H is given by (in atomic units $m = \hbar = e = 1$)

$$H = -\frac{1}{2}\Delta + V_q(r), \quad V_q(r) = -\frac{Z}{(r^q + \beta^q)^{\frac{1}{q}}}. \tag{1}$$

introduces the family of soft-core (truncated) Coulomb potentials, V_q, useful as model potentials in atomic physics. The bound states are obtained in terms of three potential parameters: the coupling $Z > 0$, the cutoff parameter $\beta > 0$, and the power parameter $q \geq 1$. The specific potentials corresponding to $q = 1$ and $q = 2$ have been analyzed earlier [1, 2, 3, 4, 5, 6, 7, 8, 9]. The potential V_1 represents the potential due to a smeared charge and may be useful in describing mesonic atoms. The potential V_2 is similar to the shape of the potential due to a finite nucleus and experienced by the muon in a muonic atom. Extensive applications of the soft-core Coulomb potential, V_2, have been made through model calculations to describe the interaction of intense laser fields with atoms [10, 11, 12, 13, 14, 15, 16, 17]. The parameter β can be related to the strength of the laser field, with the range $\beta = 20 - 40$ covering the experimental laser field strengths [10]. Mehta and Patil [1] have presented analytical solutions for the s-state eigenvalues corresponding to the V_1 potential. Patil [2] has also discussed the analyticity of the scattering phase shifts for two particles interacting through the potentials V_q with $q = 1$ and $q = 2$. Singh et al [3] have reported a large number of eigenvalues for the states $1s$ to $4f$ corresponding to V_1 and V_2 for a fixed value of Z; these values were obtained by the numerical solution of Eq.(1) for $Z = 1$; scaling laws, to be discussed here in section 2, extend their application to other values of Z. These authors noted that the energy-level ordering satisfied the condition $E_{\nu\ell} > E_{\nu\ell'}$, where $\ell < \ell'$. In these formulas, ν is the 'principal quantum number', defined generally (also for non-Coulombic potentials) as $\nu = n + \ell$, where n is the number of radial nodes plus one. For each ℓ value, the

calculated energies were found to be well represented by a Ritz type formula. Exact bound-state solutions of V_1 have been considered earlier [4, 5, 6, 7], wherein only a limited number of states with a specific choice of $\ell = 0 \dots 3$ have been treated. To our knowledge, no such study for $q \geq 2$ has been reported so far. Further, the interesting possibility of realizing the condition $E_{\nu\ell} \equiv E_{\nu'\ell'}$ at a common value of β when $\nu' > \nu$, and $\ell \neq \ell'$ has not been considered as yet, for any V_q . In view of these observations based on the review of the previous work reported on V_q, we have carried out a general analysis of the characteristic features of the energies and wave functions of the complete family of soft-core Coulomb potentials defined by V_q as a function of *all* its parameters. Next, the potential envelope method [18] is employed to express approximate estimates of $E_{\nu\ell}$ showing an interesting geometric property for all V_q. Our choice of the Asymptotic Iteration Method (AIM) [19, 20, 21, 22, 23, 24, 25, 26, 27, 28] enables us to present *general* new analytical results on exact bound-state solutions corresponding to V_1. It is then shown analytically that the electron density near the nucleus generated from all V_q is *always* concave. Finally, the first numerical results, on the crossing of energy levels in the energy spectrum corresponding to V_q, with $q = 1$ and $q = 2$ are reported. The paper is organized as follows: scaling and montonicity laws are established in sections 2 and 3; analytical spectral bounds are found by means of envelope methods in section 4; in sections 5 to 7 the Asymptotic Iteration Method is summarized and used for the case $q = 1$ to find exact analytical expressions for both eigenvalues and wave functions; in section 8 the concavity of the scaled electron density is established for all $q \geq 1$; in section 9 we discuss the characteristics of the crossings of the energy levels for soft-core Coulomb potentials, and also some comparisons of these results with those for atoms confined inside an impenetrable sphere.

II.   SCALING

The radial equation corresponding to (1) may be written

$$H\psi(r) = -\frac{1}{2}\psi''(r) + \left(\frac{\ell(\ell+1)}{2r^2} - \frac{Z}{(r^q + \beta^q)^{\frac{1}{q}}} \right)\psi(r) = E\psi(r), \tag{2}$$

where $\psi(0) = 0$. We shall take Z to be a positive real parameter and express the general parametric dependence of the eigenvalues in the form $E = E_{\nu\ell}(Z, \beta, q)$, in which, as we have noted above, for a given ℓ, the 'principal quantum number' ν is defined by $\nu = n + \ell$, where n is the number of radial nodes plus one. If we make the change of variables $r \to \sigma r$ in (2), where $\sigma > 0$ is constant, multiply through by σ^2, and compare eigenvalues, we immediately arrive at the general scaling law for this class of potentials, namely:

$$E(Z, \beta, q) = \frac{1}{\sigma^2} E(\sigma Z, \beta/\sigma, q). \tag{3}$$

The two special cases $\sigma = 1/Z$ and $\sigma = \beta$ then yield, respectively, the special scaling laws

$$E(Z, \beta, q) = Z^2 E(1, Z\beta, q) = \frac{1}{\beta^2} E(Z\beta, 1, q). \tag{4}$$

The parameter q is not involved because the denominator of the potential always scales like length, for every $q > 0$.

III.   MONOTONICITIES

The eigenvalues $E_{\nu\ell} = E(Z, \beta, q)$ are montone in each of the three potential parameters. In fact we shall now show:

$$\frac{\partial E}{\partial Z} < 0, \quad \frac{\partial E}{\partial \beta} > 0, \quad \text{and} \quad \frac{\partial E}{\partial q} < 0. \tag{5}$$

The Schrödinger operator H is bounded below. This may be shown by an application of the operator inequality [29, 30] $-\Delta > 1/(4r^2)$ which yields the general spectral bound $E > \min_{r>0}[1/(8r^2) + V(r)]$.. Explicit upper and lower bounds for all the eigenvalues may be expressed in this form with the aid of the 'potential envelope method' [18, 31, 32, 33, 34, 35, 36]; this will be discussed in the next section. Thus the discrete spectrum of H may be characterized variationally, and from this it follows that monotonicities in the potential's dependence on the parameters induces the same monotonicities in the eigenvalues. We therefore prove (5) by establishing, in turn, the corresponding monotonicities in the potential. First, by inspection, we see immediately that $\partial V/\partial Z < 0$. In what follows it is convenient to write $V(r) = -Z/F(r)$, and to note that, if s is a potential parameter, then

$$\frac{\partial V}{\partial s} = \frac{Z}{F^2(r)} \frac{\partial F}{\partial s}.$$

Thus $\partial V/\partial s$, $\partial F/\partial s$, and $\partial G/\partial s$ have the same sign, where $G(r) = \ln(F(r))$ is given by

$$G(r) = \frac{1}{q}\ln(r^q + \beta^q).$$

We see that $\partial G/\partial \beta = \beta^{q-1}/(r^q + \beta^q) > 0$; hence we have $\partial E/\partial \beta > 0$. Finally, we consider $\partial G/\partial q$. We first suppose that $r < \beta$ and we define $x = r/\beta < 1$. In terms of this new variable we find

$$\frac{\partial G}{\partial q} = -\frac{1}{q^2}\ln(1 + x^q) + \frac{1}{q}\left(\frac{x^q \ln(x)}{1 + x^q}\right).$$

Since $0 < x < 1$, it follow that $\partial G/\partial q < 0$ for $r < \beta$. An exactly analogous argument with $y = \beta/r$ for $r \geq \beta$ shows that $\partial G/\partial q < 0$ when $r \geq \beta$. Thus we conclude that $\partial E/\partial q < 0$. We note parenthetically that this result is in contrast to a generalized mean $M(q)$ of r and β given, for example, by

$$M(q) = \left(\frac{r^q + \beta^q}{2}\right)^{\frac{1}{q}}.$$

Such a mean is known [37] to be montone *increasing* in q: the '2' in the denominator of the expression for $M(q)$ makes the difference.

The analysis of the monotonicity of the potential with respect to q may be used to find the limiting potential as $q \to \infty$. We have for $r < \beta$ and $x = r/\beta < 1$,

$$\lim_{q\to\infty} G(r) = \lim_{q\to\infty}\left[\ln(\beta) + \frac{\ln(1 + x^q)}{q}\right] = \ln(\beta).$$

Similarly, for $r \geq \beta$ and $y = \beta/r \leq 1$, we find

$$\lim_{q\to\infty} G(r) = \lim_{q\to\infty}\left[\ln(r) + \frac{\ln(1 + y^q)}{q}\right] = \ln(r).$$

We conclude

$$\lim_{q\to\infty} V(r) = V_\infty(r) = \begin{cases} -\frac{Z}{\beta}, & \text{if } r < \beta; \\[2mm] -\frac{Z}{r}, & \text{if } r \geq \beta. \end{cases} \tag{6}$$

Thus, for given Z and β, the family of potentials $\{V(r)\}_{q=1}^{\infty}$ has an ordered set of graphs, of which $V_\infty(r)$ is the lowest: they intersect only at $r = 0$. For $Z = \beta = 1$, the family of potentials is illustrated in Fig. (1).

IV.   ENERGY BOUNDS BY THE 'POTENTIAL ENVELOPE METHOD'

As we mentioned above, the operator inequality $-\Delta > 1/(4r^2)$ proved in Refs. [29, 30] immediately yields a lower energy bound that is expressed by a classical formula, namely

$$E > \min_r\left[\frac{1}{8r^2} + V(r)\right].$$

The potential envelope method allows us to construct tighter and more specific energy formulas of this type. The method explores the idea that, if a given potential $V(r)$ can be written as a smooth transformation $V(r) = g(h(r))$ of a potential $h(r)$, for which the spectral problem is solved, then the Schrödinger spectrum generated by $V(r)$ may be expressed in terms of the spectrum associated with the basis potential $h(r)$. The method was introduced [18] in 1980 as a technique for the many-body problem and has subsequently been developed and used also for single-particle problems [31, 32, 33], including the laser-dressed potential [34], which we call $V_2(r)$ in the present article, and for relativistic problems [35, 36]. If the transformation function $g(h)$ is convex, the method yields lower energy bounds; conversely, when $g(h)$ is concave, the results are upper bounds. If the basis $h(r)$ of the transformation is a pure power $h(r) = \text{sgn}(p)\, r^p$, then the resulting energy formula has the form

$$E_{\nu\ell} = \min_{r>0}\left[\frac{P_{\nu\ell}^2(p)}{2r^2} - \frac{Z}{(r^q + \beta^q)^{\frac{1}{q}}}\right], \tag{7}$$

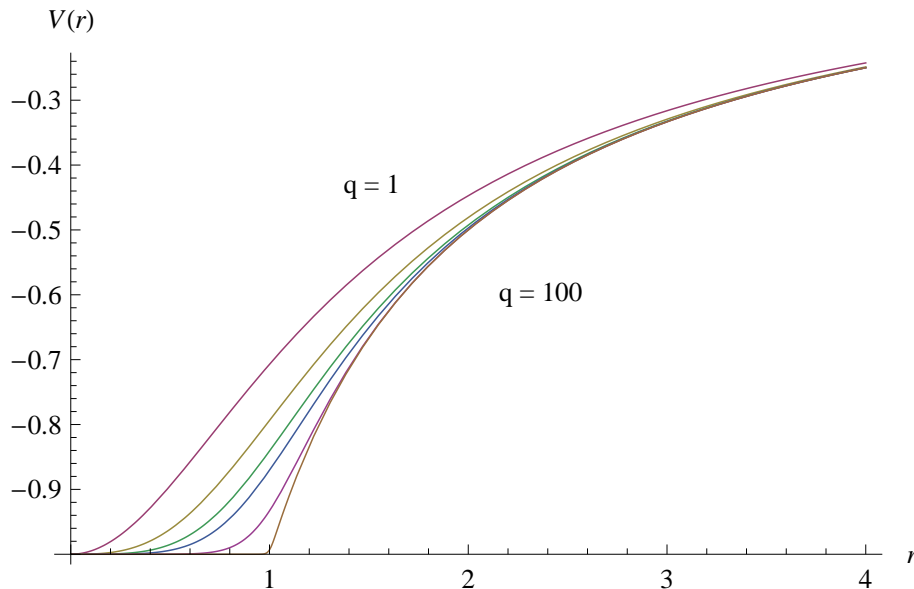FIG. 1: The family of potentials $V(r) = -1/(r^q + 1)^q$ for $1 \leq q < \infty$ (in $a.u.$). The graphs are non-intersecting for $r > 0$, and are ordered, decreasing as q increases.

where $P_{\nu\ell}(p)$ is a constant determined by $h(r)$. For the class of soft-core Coulomb potentials $V_q(r)$ we study here, we are able to obtain lower bounds if $h(r) = -1/r$, and upper bounds if $h(r) = r^2$. With the Hydrogenic basis $p = -1$, $g(h)$ is convex for all $q \geq 1$, and $P_{\nu\ell}(-1) = \nu$. For the oscillator basis $p = 2$, we have $P_{\nu\ell}(2) = 2\nu - (\ell + \frac{1}{2})$ and the transformation $g(h)$ is concave for $q <= 2$; for larger q, in this case, the formula (7) yields an upper bound provided the critical $r = \hat{r}$ found is not too small, namely for $q = \{3, 4, 5, 6\}$, respectively, we require $\hat{r}/\beta \geq \{0.958, 1.233, 1, 356, 1.417\}$. This condition arises because, even though $g(h)$ in this case ($h = r^2$, $q > 2$) is not concave everywhere, tangential potentials of the form $a + br^2$, which touch in the concave region, can still provide upper bounds provided they do not cross $V_q(r) = g(r^2)$. These energy bounds are in effect exploratory tools. The bounds obey the same scaling and monotonicity properties as the exact eigenvalues. It is perhaps geometrically interesting that the entire set of upper and lower approximate energy curves, expressing E as a function of the coupling Z, are magnifications of a single curve, with magnification factor P^2: if we write $V_q(r) = Zf(r)$, then the parametric equations for the energy-bound curves are given by

$$
\begin{cases}
Z = P^2 \left[\frac{1}{r^3 f'(r)} \right] \\[2ex]
E = P^2 \left[\frac{1}{2r^2} + \frac{f(r)}{r^3 f'(r)} \right].
\end{cases}
\tag{8}
$$

V. THE ASYMPTOTIC ITERATION METHOD

The asymptotic iteration method (AIM) was original introduced [19] to investigate the solutions of differential equations of the form

$$
y'' = \lambda_0(r)y' + s_0(r)y, \qquad ('= \frac{d}{dr})
\tag{9}
$$

where $\lambda_0(r)$ and $s_0(r)$ are $C^\infty-$differentiable functions. A key feature of this method is to note the invariant structure of the right-hand side of (9) under further differentiation. Indeed, if we differentiate (9) with respect to r, we obtain

$$
y''' = \lambda_1 y' + s_1 y
\tag{10}
$$

where $\lambda_1 = \lambda_0' + s_0 + \lambda_0^2$ and $s_1 = s_0' + s_0\lambda_0$. If we find the second derivative of equation (9), we obtain

$$
y^{(4)} = \lambda_2 y' + s_2 y
\tag{11}
$$

where $\lambda_2 = \lambda'_1 + s_1 + \lambda_0\lambda_1$ and $s_2 = s'_1 + s_0\lambda_1$. Thus, for $(n+1)^{th}$ and $(n+2)^{th}$ derivative of (9), $n = 1, 2, \ldots$, we have

$$y^{(n+1)} = \lambda_{n-1}y' + s_{n-1}y \tag{12}$$

and

$$y^{(n+2)} = \lambda_n y' + s_n y \tag{13}$$

respectively, where

$$\lambda_n = \lambda'_{n-1} + s_{n-1} + \lambda_0\lambda_{n-1} \quad \text{and} \quad s_n = s'_{n-1} + s_0\lambda_{n-1}. \tag{14}$$

From (12) and (13) we have

$$\lambda_n y^{(n+1)} - \lambda_{n-1}y^{(n+2)} = \delta_n y \quad \text{where} \quad \delta_n = \lambda_n s_{n-1} - \lambda_{n-1}s_n. \tag{15}$$

Clearly, from (15) if y, the solution of (9), is a polynomial of degree n, then $\delta_n \equiv 0$. Further, if $\delta_n = 0$, then $\delta_{n'} = 0$ for all $n' \geq n$. In an earlier paper [19] we proved the principal theorem of the Asymptotic Iteration Method (AIM), namely

Theorem 1: *Given λ_0 and s_0 in $C^\infty(a, b)$, the differential equation (9) has the general solution*

$$y(r) = \exp\left(-\int^r \alpha(t)dt\right)\left[C_2 + C_1 \int^r \exp\left(\int^t (\lambda_0(\tau) + 2\alpha(\tau))d\tau\right)dt\right] \tag{16}$$

if for some $n > 0$

$$\frac{s_n}{\lambda_n} = \frac{s_{n-1}}{\lambda_{n-1}} \equiv \alpha. \tag{17}$$

VI.   EXACT ENERGY EIGENVALUES

Since the earlier work of Ciftci et al [19], AIM has been adopted to investigate a wide range of different problems in relativistic and non-relativistic quantum mechanics. It should be noted that, in the process of applying AIM, especially to eigenvalue problems of Schrödinger-type, such as (2), one has to overcome the following two problems [20].

A.   Asymptotic Solution Problem

This problem deals with the conversion of the eigenvalue problem (the absence of first derivative) to standard form (9) suitable for the application of AIM. A general strategy to overcome this problem is to use $\psi(r) \equiv \psi_a(r)f(r)$ where $\psi_a(r)$ is an asymptotic solution satisfying the boundary conditions of the given eigenvalue equation and $f(r)$ is an unknown function to be determine using AIM. For (2), we note that, as r approaches ∞, the asymptotic solution $\psi_\infty(r)$ of (2) satisfies the differential equation

$$\psi''_\infty(r) \approx -2E\psi_\infty(r), \tag{18}$$

which yields

$$\psi_\infty(r) \approx e^{-\sqrt{-2E}r}. \tag{19}$$

Meanwhile, as r approaches 0, the asymptotic solution $\psi_0(r)$ of (2) satisfies the differential equation

$$-\psi''_0(r) + \frac{\ell(\ell+1)}{r^2}\psi_0(r) \approx 0, \tag{20}$$

which assumes the solution

$$\psi_0(r) \approx r^{l+1}. \tag{21}$$

Consequently, we may write the exact solution of (2) as

$$\psi(r) = r^{l+1} e^{-\sqrt{-2E}r} f(r). \tag{22}$$

Substituting (22) into the Schrödinger equation (2), we find that the radial function $f(r)$ must satisfy the differential equation

$$f''(r) = 2\left(a - \frac{l+1}{r}\right) f'(r) + \left(\frac{2(l+1)a}{r} - \frac{2Z}{(r^q + \beta^q)^{\frac{1}{q}}}\right) f(r) \tag{23}$$

where we denote

$$a^2 = -2E. \tag{24}$$

AIM is then used to solve this second-order homogeneous differential equation for $f(r)$.

B. Termination Condition Problem

This problem results when the eigenvalue problem (now in the standard form for an AIM application) fails to be exactly solvable. Indeed, if the eigenvalue problem has exact analytic solutions, the termination condition (17), or equivalently,

$$\delta_n(r; E) = \lambda_n(r; E)s_{n-1}(r; E) - \lambda_{n-1}(r; E)s_n(r; E) \equiv 0 \tag{25}$$

produces, at each iteration, an expression that is independent of r. For example, if $\beta = 0$, Eq.(23) is exactly solvable and the termination condition (25) yields

$$\delta_n(E) = \prod_{k=0}^{n+1} (-Z + (k+l)a), \quad n = 1, 2, \ldots \tag{26}$$

Thus the AIM condition $\delta_n(E) = 0$ leads to

$$E_n = -\frac{1}{2}\frac{Z^2}{(n+l)^2}, \quad n = 1, 2, \ldots, \tag{27}$$

as expected for the exact solutions of Coulomb potential. For $\beta \neq 0$, Eq.(23) is not exactly solvable in general, however, for certain values of the potential parameters, we can obtain some analytic solutions. For example, in the case of $q = 1$, we may use AIM with

$$\lambda_0 = 2\left(a - \frac{l+1}{r}\right), \quad s_0 = \left(\frac{2(l+1)a}{r} - \frac{2Z}{r+\beta}\right), \tag{28}$$

to obtain a class of exact solutions given by

$$a = \frac{Z}{l+n+1}, \tag{29}$$

where $n = 1, 2, 3, \ldots$ is the iteration number used by AIM, along with the conditions on the potential parameter β reported in Table 1.

TABLE I: Exact solutions of the radial Schrödinger equation (2) for $q = 1$.

a	Conditions on β
$\frac{Z}{l+2}$	$-Z\beta + l + 2 = 0$
$\frac{Z}{l+3}$	$Z^2(l+2)\beta^2 - 3Z(l+2)(l+3)\beta + (2l+3)(l+3)^2 = 0$
$\frac{Z}{l+4}$	$-Z^3(l+3)(l+2)\beta^3 + 6Z^2(l+4)(l+3)(l+2)\beta^2 - Z(11l^2 + 50l + 54)(l+4)^2\beta$ $+3(l+2)(2l+3)(l+4)^3 = 0$
$\frac{Z}{l+5}$	$Z^4(l+4)(l+3)(l+2)\beta^4 - 10Z^3(l+5)(l+4)(l+3)(l+2)\beta^3$ $+Z^2(35l^3 + 300l^2 + 823l + 720)(l+5)^2\beta^2 - Z(50l^3 + 381l^2 + 925l + 720)(l+5)^3\beta$ $+6(2l+5)(2l+3)(l+2)(l+5)^4 = 0$
$\frac{Z}{l+6}$	$-Z^5(l+5)(l+4)(l+3)(l+2)\beta^5 + 15Z^4(l+6)(l+5)(l+4)(l+3)(l+2)\beta^4$ $-Z^3(85l^4 + 1155l^3 + 5678l^2 + 11928l + 9000)(l+6)^2\beta^3$ $+3Z^2(75l^4 + 952l^3 + 4359l^2 + 8522l + 6000)(l+6)^3\beta^2$ $-Z(274l^4 + 3073l^3 + 12411l^2 + 21492l + 13500)(l+6)^4\beta$ $+30(2l+5)(2l+3)(l+3)(l+2)(l+6)^5 = 0$
$\frac{Z}{l+7}$	$Z^6(l+6)(l+5)(l+4)(l+3)(l+2)\beta^6 - 21Z^5(l+7)(l+6)(l+5)(l+4)(l+3)(l+2)\beta^5$ $+Z^4(175l^5 + 3430l^4 + 26033l^3 + 95354l^2 + 167976l + 113400)(l+7)^2\beta^4$ $-3Z^3(245l^5 + 4592l^4 + 33271l^3 + 116224l^2 + 195300l + 126000)(l+7)^3\beta^3$ $+Z^2(1624l^5 + 28182l^4 + 188607l^3 + 608332l^2 + 945783l + 567000)(l+7)^4\beta^2$ $-9Z(196l^5 + 3004l^4 + 17753l^3 + 50746l^2 + 70301l + 37800)(l+7)^5\beta$ $+90(2l+7)(2l+5)(2l+3)(l+3)(l+2)(l+7)^6 = 0$
$\frac{Z}{l+8}$	$-Z^7(l+7)(l+6)(l+5)(l+4)(l+3)(l+2)\beta^7 + 28Z^6(l+8)(l+7)(l+6)(l+5)(l+4)(l+3)(l+2)\beta^6$ $-2Z^5(161l^6 + 4284l^5 + 46109l^4 + 256284l^3 + 773558l^2 + 1198080l + 740880)(l+8)^2\beta^5$ $+2Z^4(980l^6 + 25263l^5 + 263144l^4 + 1414449l^3 + 4127804l^2 + 6184116l + 3704400)(l+8)^3\beta^4$ $-Z^3(6769l^6 + 165501l^5 + 1632238l^4 + 8299620l^3 + 22916602l^2 + 32533488l + 18522000)(l+8)^4\beta^3$ $+2Z^2(6566l^6 + 148023l^5 + 1343681l^4 + 6287868l^3 + 16004408l^2 + 21011364l + 11113200)(l+8)^5\beta^2$ $-9Z(1452l^6 + 28968l^5 + 232875l^4 + 968195l^3 + 2199048l^2 + 2589112l + 1234800)(l+8)^6\beta$ $+630(2l+7)(2l+5)(2l+3)(l+4)(l+3)(l+2)(l+8)^7 = 0$
$\frac{Z}{l+9}$	$Z^8(l+8)(l+7)(l+6)(l+5)(l+4)(l+3)(l+2)\beta^8 - 36Z^7(l+9)(l+8)(l+7)(l+6)(l+5)(l+4)(l+3)(l+2)\beta^7$ $+6Z^6(91l^7 + 3150l^6 + 45472l^5 + 354060l^4 + 1601869l^3 + 4198770l^2 + 5883828l + 3386880)(l+9)^2\beta^6$ $-18Z^5(252l^7 + 8519l^6 + 120015l^5 + 911495l^4 + 4021353l^3 + 10279346l^2 + 14054940l + 7902720)(l+9)^3\beta^5$ $+3Z^4(7483l^7 + 243355l^6 + 3294188l^5 + 24020450l^4 + 101717325l^3 + 249667695l^2 + 328201704l + 177811200)(l+9)^4\beta^4$ $-18Z^3(3738l^7 + 114755l^6 + 1464128l^5 + 10054742l^4 + 40105738l^3 + 92835203l^2 + 115350696l + 59270400)(l+9)^5\beta^3$ $+Z^2(118124l^7 + 3338080l^6 + 39154679l^5 + 247223313l^4 + 907897077l^3 + 1939695507l^2 + 2232161820l + 1066867200)(l+9)^6\beta^2$ $-18Z(6088l^7 + 152716l^6 + 1592078l^5 + 8960617l^4 + 29441156l^3 + 565025567l^2 + 58655178l + 25401600)(l+9)^7\beta$ $+2520(2l+9)(2l+7)(2l+5)(2l+3)(l+4)(l+3)(l+2)(l+9)^8 = 0$

VII. WAVE FUNCTIONS

In this section we examine the properties of the wave functions associated with the exact eigenvalues obtained in the previous section. We note first, for $a = \frac{Z}{l+2}$ and $\beta = \frac{l+2}{Z}$, the nodeless wave function of (2) is given by

$$\psi(r) = r^{l+1} \, e^{-ar} \, (1 + \frac{r}{\beta}). \tag{30}$$

Further, for $a = \frac{Z}{l+3}$, we have the following result.

Theorem: For the radial Schrödinger equation (2), if

$$\beta = \frac{(l+3)[(6+3l) + \sqrt{(2+l)(6+l)}]}{2(l+2)Z} \tag{31}$$

then the exact wave function

$$\psi(r) = r^{l+1} \, e^{-ar} \left(1 + \left(\frac{\beta(l+3)(2l+3)Z + \sqrt{\beta(l+3)^2(2l+3)Z(4(l+3)^2 - b(2l+5)Z)}}{2\beta(l+3)^2(2l+3)} \right) r \right)$$
$$\times \left(1 + \left(a - \frac{\beta(l+3)(2l+3)Z + \sqrt{\beta(l+3)^2(2l+3)Z(4(l+3)^2 - \beta(2l+5)Z)}}{2\beta(l+3)^2(2l+3)} \right) r \right), \tag{32}$$

is nodeless, while, if

$$\beta = \frac{(l+3)[(6+3l) - \sqrt{(2+l)(6+l)}]}{2(l+2)Z}, \tag{33}$$

then the exact wave function of (32) has exactly one node located at

$$r \equiv -\frac{1}{2} \frac{(l+3)(2l+3)}{(l+2)(l - \sqrt{(l+2)(l+6)})} \left[3(l+2) - \sqrt{(l+2)(l+6)} + \sqrt{2(l+2)(l+4+\sqrt{(l+2)(l+6)})} \right]. \tag{34}$$

Proof: Substitute $f(r) = (1 + sr)(1 + tr)$ in (23) and equate the coefficients of r's, we find that $a = \frac{Z}{l+3}$ and $s = a - t$ where t satisfies

$$t^2 - at + \frac{(l+2)Z^2}{(3+2l)(l+3)^2} - \frac{Z}{(3+2l)\beta} = 0.$$

Further, $f(r)$ now reads

$$f(r) = 1 + ar + (at - t^2)r^2 = 1 + ar + \left[\frac{(l+2)Z^2}{(3+2l)(l+3)^2} - \frac{Z}{(3+2l)\beta} \right] r^2.$$

From Descartes' rule of signs, $f(r)$ has no real roots if $\left[\frac{(l+2)Z^2}{(3+2l)(l+3)^2} - \frac{Z}{(3+2l)\beta} \right] > 0$ which holds for β given by (31) and has only one positive root if $\left[\frac{(l+2)Z^2}{(3+2l)(l+3)^2} - \frac{Z}{(3+2l)\beta} \right] < 0$ which holds true for β given by (33). $\square$

In Figures 2 and 3, we plot the un-normalized wave functions for $a = \frac{Z}{l+3}$ and β given by (31) and (33), respectively.
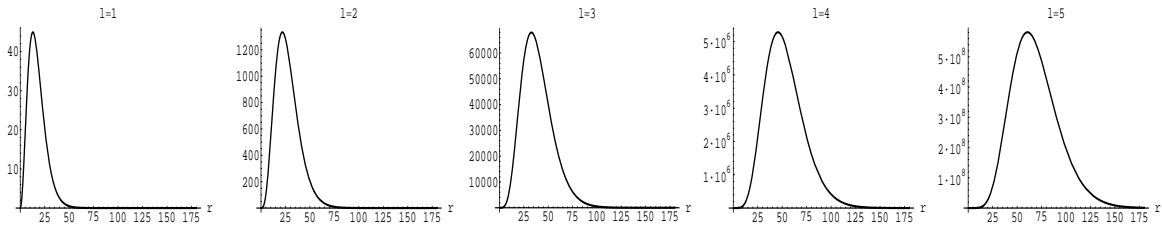

FIG. 2: Un-normalized wave functions (32) for the Schrödinger equation, Eq.(2), with soft-core Coulomb potential, $q = 1$, where $a = \frac{1}{l+3}$ and β given by (31) for different values of l (in a.u.).

Further results can be obtained similarly. Indeed, for $a = \frac{Z}{(l+4)}$, it is straightforward to show that the solution of (23) takes the form $f(r) = (1 + (a - k - t)r)(1 + kr)(1 + tr)$ with exactly no root, one root and two roots, corresponding to the positive zeros of

$$-Z^3(l+3)(l+2)\beta^3 + 6Z^2(l+4)(l+3)(l+2)\beta^2 - Z(11l^2 + 50l + 54)(l+4)^2\beta + 3(l+2)(2l+3)(l+4)^3 = 0.$$
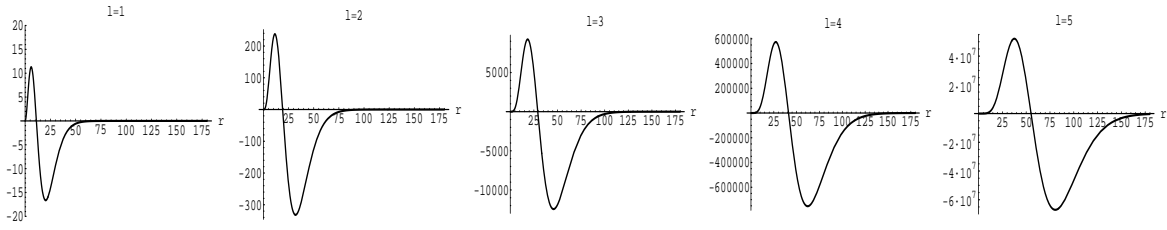
FIG. 3: Un-normalized wave functions (32) for the Schrödinger equation, Eq.(2), with soft-core Coulomb potential, $q = 1$, where $a = \frac{1}{l+3}$ and β given by (33) for different values of l (in a.u.).

VIII.   CONCAVITY OF THE SCALED ELECTRON DENSITY NEAR THE NUCLEUS

Using the radial wave function for the νl state given by

$$R_{\nu l}(r) = \frac{\psi_{\nu l}(r)}{r^{2l+1}} \ , \tag{35}$$

with the spherically averaged density normalized according to

$$4\pi \int R_{\nu l}{}^2(r) r^2 dr = 4\pi \int \overline{\varrho}(r) r^2 dr = 1 \ , \tag{36}$$

we define the *scaled* density as

$$\eta_l(r) = \frac{\overline{\varrho}(r)}{r^{2l}} \tag{37}$$

We note here that the Kato-Steiner cusp condition [38, 39, 40, 41] in terms of the density is given by

$$\eta_l'(0) = -\frac{2Z}{l+1}\eta_l(0) \tag{38}$$

Now, for a spherical potential of the form $-\frac{A}{r} + B + f(r)$, where $f(r) \to 0$ as $r \to 0$ it has been shown [42, 43] that

$$\eta_l''(0) = \frac{2}{2l+3}\left[\frac{A^2}{(l+1)^2}(4l+5) + 2(B - E_{nl})\right]\eta_l(0) \tag{39}$$

Writing the soft-core Coulomb potential as

$$V_q(r) = -\frac{Z}{\beta} + \left(\frac{Z}{\beta} - \frac{Z}{(r^q + \beta^q)^{\frac{1}{q}}}\right) = B + f(r),$$

we see that $A = 0$, $B = -Z/\beta$, and $f(0) = 0$. Thus we have from (39)

$$\eta_l''(0) = -\frac{4}{2l+3}\left[E_{\nu l} + \frac{Z}{\beta}\right]\eta_l(0) \tag{40}$$

The sign of $\eta_l''(0)$ is then completely determined by the quantity $E_{\nu l} + \frac{Z}{\beta}$. Writing

$$E_{\nu l} = (\psi_{\nu l}, H\psi_{\nu l}) = \left(\psi_{\nu l}, \left[-\frac{1}{2}\Delta + V_q(r)\right]\psi_{\nu l}\right), \tag{41}$$

we find that

$$E_{\nu l} \geq (\psi_{\nu l}, V_q(r)\psi_{\nu l}) \geq \min_r [V_q(r)] = -\frac{Z}{\beta} \tag{42}$$

Therefore, for all $V_q(r)$, $\eta''_l(0) \leq 0$ i.e. the electron density near the nucleus remains *concave*. Specifically for $V_1(r)$, the exact nodeless wave functions at $\beta = \frac{(l+2)}{Z}$ correspond to $E = -\frac{Z^2}{2(l+2)^2}$ which leads to the simple result that

$$\frac{\eta''_l(0)}{\eta_l(0)} = -\frac{2Z^2}{(l+2)^2}.$$

The corresponding ratios for the results obtained in Table I, given by AIM, can be similarly derived. Our numerical analysis on the trends in the eigenvalues for the potential $V_2(r)$, support the earlier result [16] that the nodeless wave functions with energy $E = -\frac{Z^2}{2(l+2)^2}$ are produced at $\beta = \sqrt{\frac{2(l+2)^3}{Z^2}}$. This leads to the ratio

$$\frac{\eta''_l(0)}{\eta_l(0)} = -\frac{2Z^2[\sqrt{2}(l+2)-1]}{(2l+3)(l+2)^2}.$$

Such ratios can be obtained for the other β values at which the exact energy values are known [16]. It has been argued [44, 45] that the electron density in terms of the ratio $\frac{\eta'_l(0)}{\eta_l(0)} = -\frac{2Z}{l+1}$ carries information on the identity of the nuclei, i.e., the value of Z and its location. The corresponding external potential at the equilibrium density thus provides a rationalization for the existence of the ground state energy-density functional [46]. An interesting situation arises in the case of the $V_q(r)$ class of potentials when $\eta'_l(0)$ vanishes. The information on the identity of the nuclei is then contained in the ratio $\frac{\eta''_l(0)}{\eta_l(0)}$. We conclude this section by noting that Eq.(38) can be used to obtain the condition on $\frac{\eta''_l(0)}{\eta_l(0)}$ corresponding to the critical potential at which $E_{\nu l} \equiv 0$.

IX. ENERGY DEGENERACIES FOR $\beta > 0$ AND THE CHARACTERISTICS OF ENERGY-LEVEL CROSSINGS

In this section we shall discuss the characteristic features associated with the crossings of the energy levels. Our results are derived from accurate numerical calculations carried out for $V_q(r)$, $q = 1 - 4$ over $\beta = 0 - 100$ in steps of 1. We have employed the generalized pseudo-spectral (GPS) Legendre method with mapping, which is a fast algorithm that has been tested extensively and shown to yield the eigenvalues with an accuracy of twelve digits after the decimal. A more detailed account, with several applications of GPS, can be found in [47, 48, 49, 50, 51, 52] and the references therein. In the present work, we have also verified the accuracy of these results, in a few selected cases, by using AIM. In order to discuss the characteristic features of the level crossings, it is useful to compare the soft-core Coulomb potentials with the case of hydrogen atom confined inside an impenetrable spherical cavity of radius R. The model potential for the spherically confined hydrogen atom , SCHA, [53] is given by $V_{SCHA}(r) = -\frac{Z}{r}$ for $r < R$; $and = \infty$ for $r \geq R$. The choice of parameters, $R = \infty$ and $\beta = 0$ in the potentials $V_{SCHA}(r)$ and $V_q(r)$ reduce them to that of the free hydrogen-like atom which is characterised by the well known accidental degeneracy of energy levels. At finite values of the parameters, the accidental degeneracy is lifted for the two potentials. The relative ordering of (ν, l), however, has a different functional dependence on the parameters. We note here that the level ordering for $V_q(r)$ is similar to that of muonic atoms where the state with angular momentum $(l+1)$ is more strongly bound than the one with l which is different from the aufbau principle corresponding to the neutral atoms in the periodic table. For the two potentials $V_{SCHA}(r)$ and $V_q(r)$, the higher l states get relatively less destabilized as β or $\frac{1}{R}$ increases (that is to say, the eigenvalues *decrease*). These properties, in conjunction with the property of monotonicity, give rise to the crossing of a pair of states $[(\nu, \ell) \, (\nu', \ell')]$ with $\nu' > \nu$, $l' > l$ which are different for $V_{SCHA}(r)$ and $V_q(r)$. In general, such crossings produce new degeneracy conditions not present in the free atom. In the SCHA, the *simultaneous degeneracy* condition [54, 55] is obtained such that *all* $\nu \geq \ell + 2$, each (ν, ℓ) SCHA state is degenerate with $(\nu + 1, \ell + 2)$ state, when both of them are confined at $R = (\ell + 1)(\ell + 2)$. The latter defines the radial node in the free $(\ell + 2, \ell)$ state. For example, at $R = 2 \, a.u.$, *all* pairs of states $(2s, 3d), (3s, 4d), ...$ become *simultaneously* degenerate. For the soft-core Coulomb potential, $V_q(r)$, our numerical analysis shows that (a) the crossing takes place at a certain β between a pair of states, $[(\nu, \ell), (\nu', \ell')]$, defined by $\nu' \geq (\nu + 1)$ and $\ell' \geq (\ell + 3)$, (b) β varies as ν changes and it is not related to the location of radial nodes in the free hydrogen atom, (d) due to the muonic atom ordering, the higher than $\ell + 3$ states which lie below have already crossed over before an $[(\nu, \ell), (\nu + 1, \ell + 3)]$ level crossing occurs. In Fig. 4 we have displayed the crossings of the $6s$ level with $7f$,$7g$, and $7i$ levels given by the $V_1(r)$ potential as β is varied.

Similar level crossings are obtained in the cases of $V_q(r)$ with $q = 2 - 6$. In Fig. 5 shows the level crossings of the $(4p - 5g)$, $(5p - 6g)$, $(6p - 7g)$ and $(7p, 8g)$ pairs derived from $V_2(r)$ as a function of β. This potential gives a good approximation for the laser-dressed hydrogen atom in intense laser field, and the parameter β can be identified with
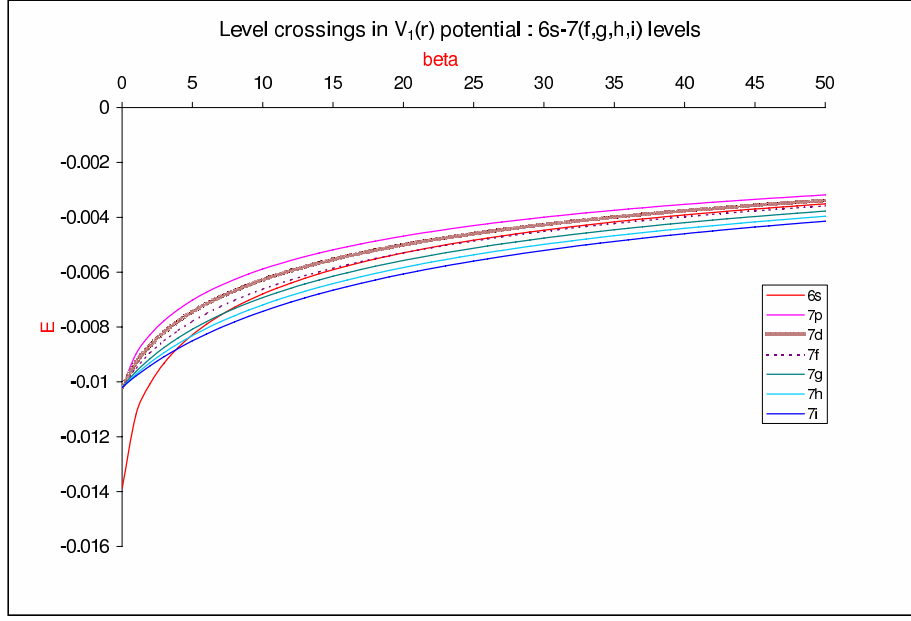
FIG. 4: Crossings of energy levels in $V_1(r) = -1/(r + \beta)$ for the $6s$ level with $7f$, $7g$, and $7i$ levels as a function of β (in $a.u.$). The energy level ordering over the range $\beta = 20 - 40$ is changed relative to that corresponding to lower β values.

the field strength. We note in Fig. 5 that the level ordering gets inverted while passing through the range of the experimentally important region defined by $\beta = 20 - 40$. In addition to their relevance in describing the interaction of intense laser fields with atoms using soft-core Coulomb potential, such theoretical predictions may have applications in the design of optical devices. Finally, as noted in $Eq.(4)$, the parameter q is not involved in the energy scaling. We have also studied numerically the variation of $E_{\nu\ell}$ as a function of q at fixed β values. We do not observe any level crossing in these energy curves.
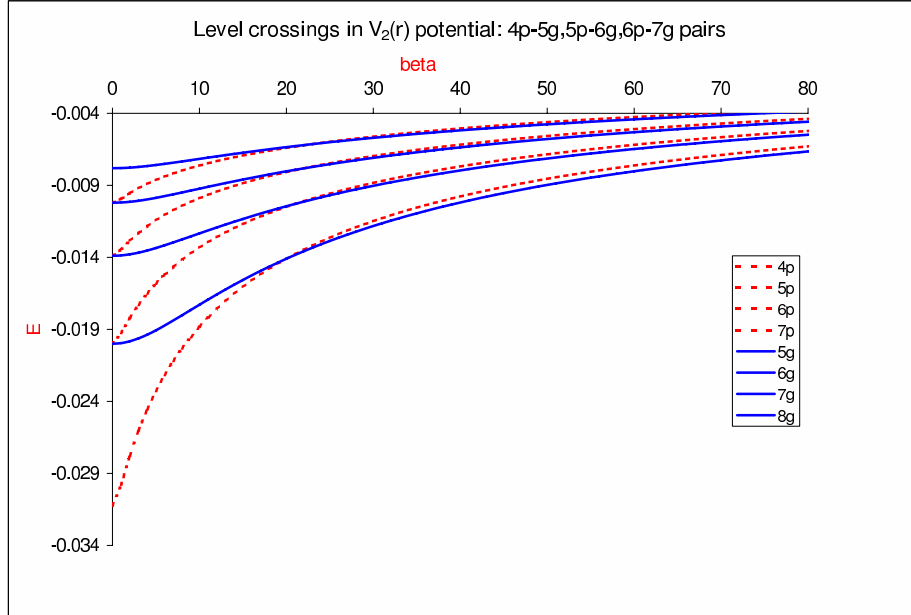

FIG. 5: Crossings of energy levels in $V_2(r) = -1/(r^2 + \beta^2)^{1/2}$ for pair of levels $(4p - 5g)$, $(5p - 6g)$, $(6p - 7g)$ as a function of β (in $a.u.$). The energy level ordering over the range $\beta = 20 - 40$ undergoes changes as a consequence of cross overs.

X. CONCLUSIONS

In this work we have obtained several novel analytic results on the behavior of energies and wave functions for a class of experimentally useful model soft-core Coulomb potentials represented by $V_q(\beta, Z, q)$. Since the Hamiltonian H is bounded below, the energy spectrum can be characterized variationally. This allows us to conclude that monotonicities of potential in the parameters $\{Z, \beta, q\}$ induces corresponding monotonicities in the eigenvalues $E_{\nu\ell}$. Upper and lower energy bounds have been derived by an application of the potential envelope method [18] wherein $V_q(r)$ is written as a smooth transformation of a monomial potential. Such bounds are found to obey the same scaling and monotonicity properties as the exact $E_{\nu\ell}$ and exhibit interesting geometric property described by a common magnification factor. The Asymptotic Iteration Method (AIM) is used for the case V_1 to provide exact analytical bound-state solutions for both eigenvalues and wave functions. We have proved that the electron density near the nucleus generated from all V_q is *always* concave. This result, along with the specific condition on β corresponding to the exact energy obtained by use of AIM for V_1, and a similar estimate, derived numerically, for V_2, suggests that the ratio $\frac{\eta_l''(0)}{\eta_l(0)}$ contains the information on the identity and location of the nuclear charge Z. Finally, the crossing of energy levels in the energy spectrum of V_q, have been analyzed using extensive numerical calculations of $E_{\nu\ell}$ as a function of β. It is conjectured that a pair of states, $[(\nu, \ell), (\nu', \ell')]$, obey the crossing condition given by $\nu' \geq (\nu + 1)$ and $\ell' \geq (\ell + 3)$. This condition is completely different from that of the hydrogen atom confined inside an impenetrable spherical cavity, where, at a characteristic common value of the radius of confinement, all such pairs of states become *simultaneously* degenerate when $\ell' = (\ell + 2)$. Finally, in the case of the potential V_2, which approximates the laser-dressed hydrogen atom potential, it is pointed out that the level crossing effects significantly alter the level ordering over the range of $\beta = 20 - 40$, that is identified with the field strengths of the experimental sources of intense laser radiation.

Acknowledgments

[1] C.H. Mehta and S.H. Patil , Phys. Rev. A **17**, 43 (1978).
[2] S.H. Patil, Phys. Rev. A **24**, 2913 (1981).
[3] D. Singh, Y. P. Varshni and R. Dutt, Phys. Rev. A **32**, 619 (1985).
[4] H. De Meyer and G. Vanden Berghe, J. Phys. A: Math. Gen. 23, 1323 (1990).
[5] A. Sinha and R. Roychoudhury, J. Phys. A: Math. Gen. **23**, 3869 (1990).
[6] F. M. Fernández, J. Phys. A: Math. Gen. **24**, 1351 (1991).
[7] R.N. Chaudhuri and M. Mondal, Pramana-J.Phys., **39**, 493 (1992).
[8] M. Odeh and O. Mustafa, J. Phys. A: Math. Gen. **33**,7013(2000.
[9] O. Mustafa and M. Odeh J.Phys. B: At. Mol. Opt. Phys. **32**,3055 (1999).
[10] C.A.S. Lima and L.C.M. Miranda, Phys. Rev. A **23**, 3335 (1981).
[11] J.H. Eberly, Q. Su and J. Javanainen, Phys. Rev. Lett. **62**, 881 (1989).
[12] J.H. Eberly, Phys. Rev. A **42**, 5750 (1990).
[13] Q. Su and J.H. Eberly, Phys. Rev. A **44**, 5997 (1991).
[14] R. Panfili, J.H. Eberly and S.L. Haan, Optics Express **8**, 431 (2001).
[15] M. Protopapas, C.H. Keitel and P.L. Knight, Rep. Prog. Phys. **60**, 389 (1997). References therein.
[16] C.W. Clark, J. Phys. B **30**, 2517 (1997).
[17] Y. I. Salamin, S. H. Hu, K. Z. Hatsagortsyan, C. H. Keitel, Phys. Rep. **427**, 41 (2006).
[18] R. L. Hall, Phys. Rev. D **22**,2062 (1980).
[19] H. Ciftci, R.L. Hall and N. Saad, J. Phys. A: Math. Gen.**36** 11807-11816 (2003).
[20] B. Champion, R. L. Hall, and N. Saad, Int. J. Mod. Phys. A **23** 1405-1415 (2008).
[21] M.F. Fernández, J. Phys. A: Math. Gen. **37** 6173 (2004).
[22] H. Ciftci, R.L. Hall and N. Saad, J. Phys. A: Math. Gen.**38** 1147-1155 (2005).
[23] H. Ciftci, R.L. Hall and N. Saad, Phys. Lett. A **340** 388-396 (2005).
[24] T. Barakat, Phys. Lett. A **344** 411 (2005).
[25] T. Barakat, K. Abodayeh and A. Mukheimer, J. Phys. A: Math. Gen. **38** 1299 (2005).

[26] T. Barakat, J. Phys. A: Math. Gen. **39** 823-831 (2006).
[27] O. Bayrak and I. Boztosun I, J. Phys. A: Math. Gen. **39** 6955 (2006).
[28] N. Saad, R.L. Hall and H. Ciftci, J. Phys. A: Math. Gen. **39** 8477-8486 (2006).
[29] M. Reed and B. Simon, *Methods of modern mathematical physics II: Fourier analysis and self-adjointness*, (Academic Press, New york, 1975). [The operator inequality is proved on p 169].
[30] S. J. Gustafson and I. M. Sigal, *Mathematical concepts of quantum mechanics*, (Springer, New York, 2006). [The operator inequality is proved for dimensions $d \geq 3$ on page 32.]
[31] R. L. Hall, J. Math. Phys. **24**, 324 (1983).
[32] R. L. Hall, J. Math. Phys. **25**, 2708 (1984).
[33] R. L. Hall, J. Math. Phys. **34**, 2779 (1993).
[34] J. Paul Duarte and R. L. Hall, J. Phys. B **27**, 1021 (1994).
[35] R. L. Hall, Phys. Rev. Lett. **83**, 468 (1999).
[36] R. L. Hall, W. Lucha, and F. F. Schöberl, Int. J. Mod. Phys. A **17**, 1931 (2002).
[37] G. H. Hardy, J. E. Littlewood, and G. Pólya, *Inequalities*, (Cambridge University Press, Cambridge, 1952). The monotonicity of the general mean is discussed on page 26.
[38] T. Kato, Commun. Pure Appl. Math. **10**, 151 (1957).
[39] E. Steiner, J. Chem. Phys. **39**, 2365 (1963).
[40] R.T. Pack and W.B. Brown, J. Chem. Phys. **45**, 556 (1966).
[41] A. Nagy and K.D. Sen, J. Phys. B:At. Mol. Opt. Phys. **33**, 1745 (2000).
[42] H.E. Montgomery Jr. and K.D. Sen, Int. J. Quantum Chem. **109**, 688 (2009).
[43] K.D. Sen, V. I. Pupyshev and H.E. Montgomery Jr., Ad. Quantum Chem. **57**, 25 (2009).
[44] E.B. Wilson, *Structural chemistry and biology*, Eds: A. Rich and N. Davidson (Freeman, San Francisco, CA, 1968).
[45] N.C. Handy, Mol. Phys. **107**, 721 (2009).
[46] P. Hohenberg and W. Kohn, Phys. Rev. **136**, B864 (1964).
[47] G. Yao and S. I. Chu, Chem. Phys. Lett. **204**, 381 (1993).
[48] J. Wong, S. I. Chu and C. Laughlin, Phys. Rev. A **50**, 3208 (1994).
[49] X. M. Tong and Shih-I. Chu, Phys. Rev. A **64**, 013417 (2001).
[50] A. K. Roy and Shih-I. Chu, Phys. Rev. A **65**, 043402 (2002). *ibid.* **65**, 052508 (2002).
[51] K.D. Sen and A.K. Roy, Phys. Lett. A. **357**, 112 (2006).
[52] H.E. Montgomery Jr., N.A. Aquino and K.D. Sen, Int. J. Quantum Chem. **107**, 798 (2007).
[53] A. Michels, J. de Boer and A. Bijl, Physica **4**, 981 (1937).
[54] A. I. Pupyshev and A. V. Scherbinin, Chem. Phys. Lett. **295**, 217 (1998).
[55] A. I. Pupyshev and A. V. Scherbinin, Phys. Lett. A **299**, 371 (2002).